# Viral dynamics in human immunodeficiency virus type 1 infection

**Xiping Wei[*], Sajal K. Ghosh[*], Maria E. Taylor[*], Victoria A. Johnson[†], Emilio A. Emini[‡], Paul Deutsch[§], Jeffrey D. Lifson[‖], Sebastian Bonhoeffer[¶], Martin A. Nowak[¶], Beatrice H. Hahn[*], Michael S. Saag[†] & George M. Shaw[*#]**

Divisions of * Hematology/Oncology and † Infectious Diseases, University of Alabama at Birmingham, 613 Lyons-Harrison Research Building, 701 South 19th Street, Birmingham, Alabama 35294, USA
Departments of ‡ Antiviral Research and § Clinical Pharmacology, Merck Research Laboratories, West Point, Pennsylvania 19486, USA
‖ Division of HIV and Exploratory Research, Genelabs Technologies Inc., Redwood City, California 94063, USA
¶ Department of Zoology, University of Oxford, Oxford OX1 3PS, UK

**The dynamics of HIV-1 replication *in vivo* are largely unknown yet they are critical to our understanding of disease pathogenesis. Experimental drugs that are potent inhibitors of viral replication can be used to show that the composite lifespan of plasma virus and virus-producing cells is remarkably short (half-life ~2 days). Almost complete replacement of wild-type virus in plasma by drug-resistant variants occurs after fourteen days, indicating that HIV-1 viraemia is sustained primarily by a dynamic process involving continuous rounds of *de novo* virus infection and replication and rapid cell turnover.**

THE natural history and pathogenesis of human immunodeficiency virus type-1 (HIV-1) infection are linked closely to the replication of virus *in vivo*[1-17]. Clinical stage is significantly associated with all measures of virus load, including infectious virus titres in blood, viral antigen levels in serum, and viral nucleic acid content of lymphoreticular tissues, peripheral blood mononuclear cells (PBMCs) and plasma (reviewed in ref. 18). Moreover, HIV-1 replication occurs preferentially and continuously in lymphoreticular tissues (lymph node, spleen, gut-associated lymphoid cells, and macrophages)[11,19,20]; virus is detectable in the plasma of virtually all patients regardless of clinical stage[6,10,13,21]; and changes in plasma viral RNA levels predict the clinical benefit of antiretroviral therapy (R. Coombs, unpublished results). These findings emphasize the central role of viral replication in disease pathogenesis.

Despite the obvious importance of viral replication in HIV-1 disease, relatively little quantitative information is available regarding the kinetics of virus production and clearance *in vivo*, the rapidity of virus and $CD4^+$ cell population turnover, and the fixation rates of biologically relevant viral mutations[22,23]. This circumstance is largely due to the fact that previously available antiretroviral agents lacked sufficient potency to abrogate HIV-1 replication, and methods to quantify virus and determine its genetic complexity were not sufficiently sensitive or accurate. We overcame these obstacles by treating subjects with new investigational agents which potently inhibit the HIV-1 reverse transcriptase (nevirapine, NVP)[24] and protease (ABT-538; L-735,524)[25,26]; by measuring viral load changes using sensitive new quantitative assays for plasma virus RNA[6,18,27]; and by quantifying changes in viral genotype and phenotype in uncultured plasma and PBMCs using automated DNA sequencing[28] and an *in situ* assay of RT function[29,30].

## Virus production and clearance

Twenty-two HIV-1-infected subjects with $CD4^+$ lymphocyte counts between 18 and 251 per $mm^3$ (mean ± s.d., 102 ± 75 cells per $mm^3$) were treated with ABT-538 ($n = 10$), L-735,524 ($n = 8$) or NVP ($n = 4$) as part of phase I/IIA clinical studies. The design and clinical findings of those trials will be reported elsewhere (K. Squires *et al.*, and V.A.J. *et al.*, manuscripts in preparation). Plasma viral RNA levels in the 22 subjects at baseline ranged from $10^{4.6}$ to $10^{7.2}$ molecules per ml (geometric mean of $10^{5.5}$) and exhibited maximum declines generally within 2 to 4 weeks of initiating drug therapy (Figs 1 and 2*a*). For ABT-538- and L-735,524-treated patients, virus titres fell by as much as $10^{3.9}$-fold (mean decrease of $10^{1.9}$-fold) whereas for NVP-treated patients virus fell by as much as $10^{2.0}$-fold (mean decrease of $10^{1.6}$-fold). The overall kinetics of virus decline during the initial weeks of therapy with all three agents corresponded to an exponential decay process (Figs 1 and 2*a*).

The antiretroviral agents used in this study, despite their differing mechanisms of action, have a similar overall biological effect in that they block *de novo* infection of cells. Thus the rate of elimination of plasma virus that we measured following the initiation of therapy is actually determined by two factors: the clearance rate of plasma virus *per se* and the elimination (or suppression) rate of pre-existing, virus-producing cells. To a good approximation, we can assume that virus-producing cells decline exponentially according to $y(t) = y(0)e^{-\alpha t}$, where $y(t)$ denotes the concentration of virus-producing cells at time $t$ after the initiation of treatment and $\alpha$ is the rate constant for the exponential decline. Similarily, we assume that free virus $v(t)$ is generated by virus-producing cells at the rate $ky(t)$ and declines exponentially with rate constant $u$. Thus, for the overall decline of free virus, we obtain $v(t) = v(0)[ue^{-\alpha t} - \alpha e^{-ut}]/(u - \alpha)$. The kinetics are largely determined by the slower of the two decay processes. As we have data only for the decline of free virus, and not for virus-producing cells, we cannot determine which of the two decay processes is rate-limiting. However, the half-life ($t_{1/2}$) of neither process can exceed that of the two combined. With these considerations in mind, we estimated the elimination rate of plasma virus and of virus-producing cells by three different methods: (1) first-order kinetic analysis of that segment of the viral elimination curve corresponding to the most rapid decline in plasma virus, generally somewhere between days 3 and 14; (2) fitting of a simple exponential decay curve to all viral RNA determinations between day 0 and the nadir or inflection point (Fig. 1); and (3) fitting of a compound decay curve

# To whom correspondence should be addressed.

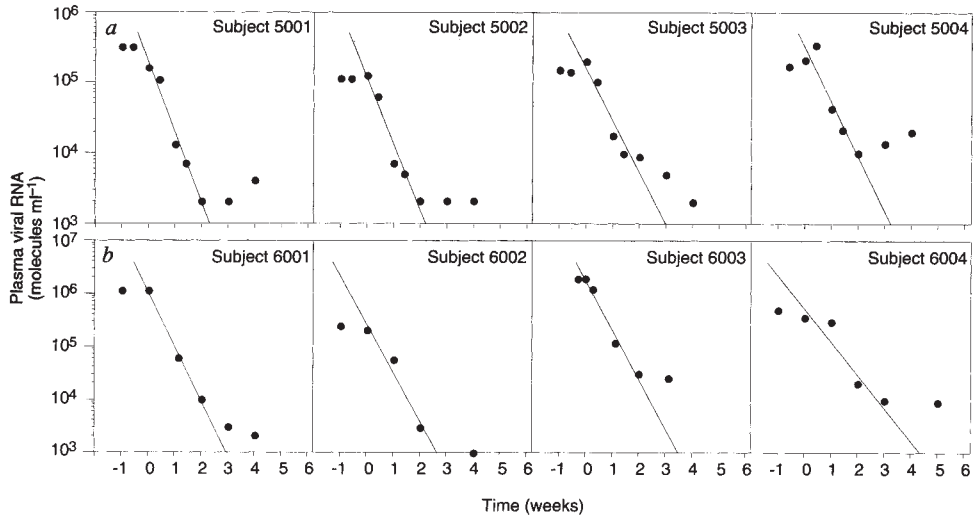


FIG. 1 Plasma viral RNA determinations in representative subjects treated with the HIV-1 protease inhibitors ABT-538 (*a*) and L-735,524 (*b*). Subjects had not received other antiretroviral agents for at least 4 weeks before therapy. Treatment was initiated at week 0 with 400–1,200 mg $d^{-1}$ of ABT-538 or 1,600–2,400 mg $d^{-1}$ of L-735,524 and was continued throughout the study. Viral RNA was determined by modified branched DNA (bDNA)[18] (*a*) or RT-PCR[27] (*b*) assay and confirmed by QC-PCR[6]. Shown are the least-squares fit linear-regression curves for data points between days 0 and 14 indicating exponential (first-order) viral elimination.

that takes into account the two separate processes of elimination of free virus and virus-producing cells, as described. Method (1) gives a $t_{1/2}$ of $1.8 \pm 0.9$ days; method (2) gives a $t_{1/2}$ of $3.0 \pm 1.7$ days; and method (3) gives a $t_{1/2}$ of $2.0 \pm 0.9$ days for the slower of the two decay processes and a very similar value, $1.5 \pm 0.5$ days, for the faster one. These are averages ($\pm 1$ s.d.) for all 22 patients. Method (3) arguably provides the most complete assessment of the data, whereas method (2) provides a simpler interpretation (but slightly slower estimate) for virus decline because it fails to distinguish the initial delay in onset of antiviral activity due to the drug accumulation phase, and the time required for very recently infected cells to initiate virus expression, from the subsequent phase of exponential virus decline. There were no significant differences in the viral clearance rates in subjects treated with ABT-538, L-735,524 or NVP, and there was also no correlation between the rate of virus clearance from plasma and either baseline $CD4^+$ lymphocyte count or baseline viral RNA level.

## Virus turnover

**Direct population sequencing.** As an independent approach for determining virus turnover and clearance of infected cells, we quantified serial changes in viral genotype and phenotype with respect to drug resistance in the plasma and PBMCs of four subjects treated with NVP (Fig. 2). NVP potently inhibits HIV-1 replication but selects for one or more codon substitutions in the reverse transcriptase (RT) gene[24,31,32]. These mutations result in dramatic decreases (up to 1,000-fold) in drug susceptibility and are associated with a corresponding loss of viral suppression *in vivo*[32]. Genetic changes resulting in NVP resistance can thus serve as a quantifiable molecular marker of virus turnover. A rapid decline in plasma viral RNA was

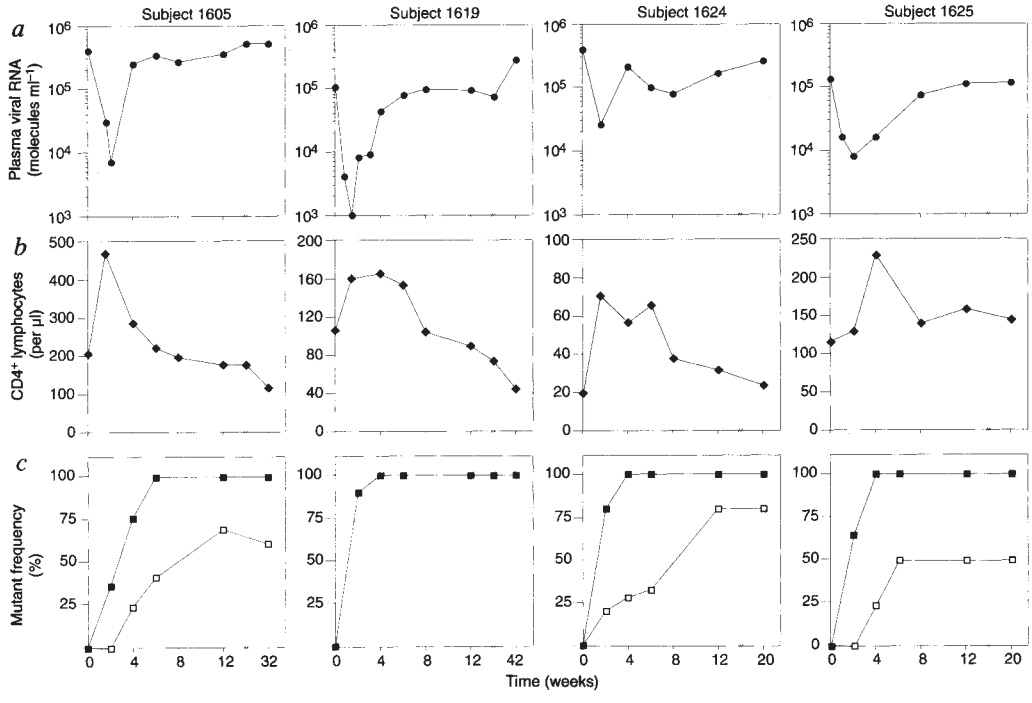


FIG. 2 Plasma viral RNA determinations (*a*), $CD4^+$ lymphocyte counts (*b*), and percentages of mutant viral genomes in plasma and PBMCs (*c*) of subjects initiating treatment with NVP. Subjects were participants in a clinical protocol assessing the effects of NVP when added to existing treatment with ddI (subject 1605) or ddI plus zidovudine (subjects 1619, 1624, 1625). Treatment with NVP was initiated at week 0 using 200 mg per day and was increased to 400 mg per day after 2 weeks. ddI and zidovudine dosages were 400 mg per day and 300–600 mg per day, respectively. Viral RNA (●) was determined by QC-PCR assay[6]. $CD4^+$ lymphocytes (◆) were quantified by flow cytometry. Frequencies of viral genomes containing NVP-resistance-associated mutations in plasma (■) and PBMCs (□) were determined by automated DNA sequence analysis (Fig. 3, legend), with each data point representing the average of 3–6 independent PCR amplifications and sequence determinations.

observed following the institution of NVP therapy and this was associated with a reciprocal increase in $CD4^+$ lymphocyte counts (Fig. 2*a* and *b*). Both responses were of limited duration, returning to baseline within 6–20 weeks in these four patients. The proportion of virus in uncultured plasma and PBMCs that contain NVP-resistance-conferring mutations (Fig. 2*c*) was determined by direct automated nucleotide sequencing of viral nucleic acid (Fig. 3), as previously described[28]. We first validated this method by reconstitution experiments, confirming its sensitivity for detecting RT mutants that comprise as little as 10% of the overall virus population. Defined mixtures of wild-type and mutant HIV-1 RT cDNA clones (differing only at the second base position of codon 190) were amplified and sequenced (Fig. 3*a*). Varying proportions of wild-type and mutant viral sequences present in the original DNA mixtures (mutant composition: 0, 10, 25, 50, 75 and 100%) were faithfully represented in the relative peak-on-peak heights (and in the relative peak-on-peak areas) of cytosine (C) and guanine (G) residues at the second base position within this codon. Ratios of (mutant)/(mutant + wild type) nucleotide peak heights expressed in arbitrary fluorescence units were as follows (predicted/observed): 0/< 10%; 10/18%; 25/29%; 50/49%; 75/71% and 100/94%.

We next determined the ability of direct population sequencing to quantify wild-type and mutant viral RNA genomes in clinical specimens. Figure 3*b* shows the sequence chromatograms of RT codons 179–191 from virions pelleted directly from uncultured plasma specimens of subject 1625 before (day −7) and after (days +28 and +140) the initiation of NVP therapy. At day −7, all codons within the amino-terminal half of the RT gene (codons 1–250), including those shown, were wild-type at positions associated with NVP resistance[31,32]. However, after only 28 days of NVP therapy, the wild-type plasma virus population was completely replaced by a NVP-resistant mutant population differing from the wild-type at codon 190 (glycine-to-serine substitution). After 140 days of drug therapy, this codon had evolved further such that the plasma virus population consisted of an equal mixture of two drug-resistant strains, one containing G190S and the other containing G190A. There were no other NVP-resistance-conferring mutations detectable within the viral RT gene.

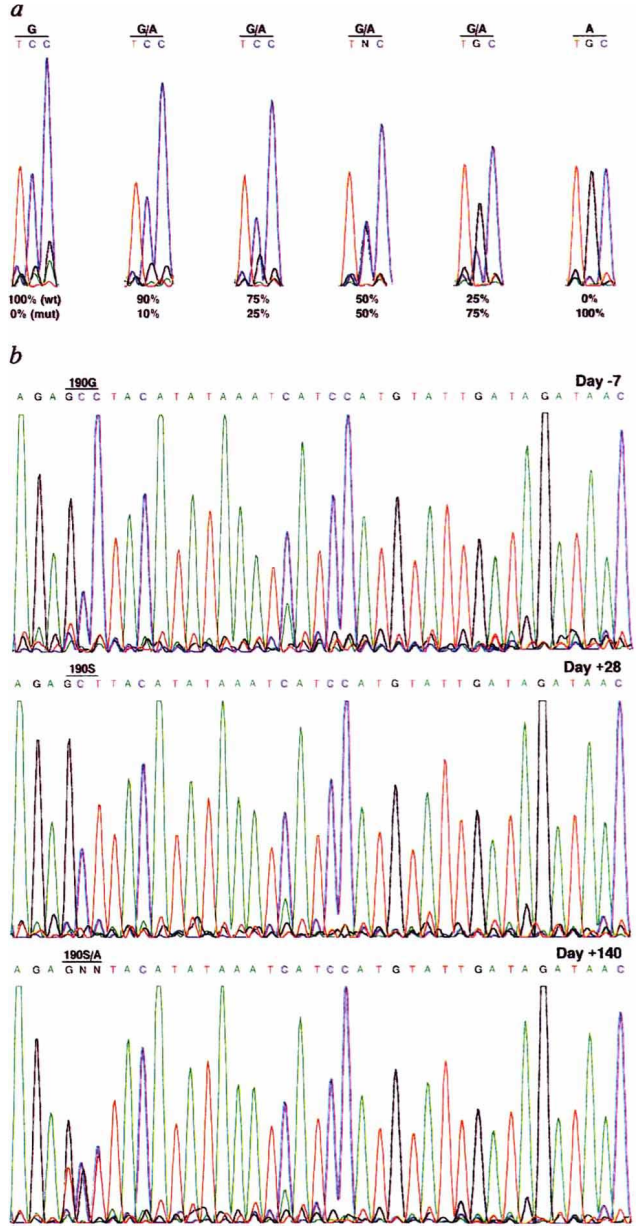


FIG. 3 Quantitative detection of HIV-1 drug-resistance mutations by automated DNA sequencing. *a*, DNA sequence chromatograms of RT codon 190 from a defined mixture of wild-type (wt) and mutant (mut) HIV-1 cDNA clones differing only at the second base position of the codon. Sequences shown were obtained from, and therefore are presented as, the minus (non-coding) DNA strand. For example, the minus-strand TCC sequence shown corresponds to the plus-strand codon GGA (glycine, G). Similarly, the minus-strand TGC sequence corresponds to the plus-strand codon GCA (alanine, A). The single-letter amino-acid code corresponds to the plus-strand DNA sequence. Mixed bases approximating a 50/50 ratio are denoted as N. *b*, DNA sequence chromatograms of RT codons 179–191 (again displayed as the minus-strand sequence) derived from plasma-virion-associated RNA of subject 1625 before (day −7) and after (days +28 and +140) starting NVP therapy. Codon changes resulting in amino-acid substitutions at position 190 are indicated for the plus strand. For example, the GCC minus-strand sequence at position 190 (day −7) corresponds to GGC (glycine, G), and the GCT minus-strand sequence at position 190 (day +28) corresponds to AGC (serine, S) in the respective plus strands.
METHODS. Mixtures of wild-type and mutant cDNA clones (*a*) were prepared and diluted such that first-round PCR amplifications were done with 1,000 viral cDNA target molecules per reaction. HIV-1 RNA was isolated from virions pelleted from uncultured plasma specimens (*b*), as described[18]. cDNA was prepared using Moloney murine leukaemia virus reverse transcriptase (GIBCO BRL)[6] and an oligonucleotide primer corresponding to nucleotides 4,283 to 4,302 of the HXB2 sequence[43]. The full-length viral reverse transcriptase gene (1,680 bp) was amplified by means of a nested PCR using conditions and oligonucleotide primers (outer primers: nt 2,483–2,502 and 4,283–4,302; inner primers: nt 2,549–2,565 and 4,211–4,229), previously reported[30]. Subgenomic fragments of the RT gene were also amplified using combinations of the following oligonucleotide primers: (5′) 2,585–2,610; (5′) 2,712–2,733; (3′) 2,822–2,844; (3′) 3,005–3,028; (3′) 3,206–3,228; (3′) 3,299–3,324; (3′) 3,331–3,350; (3′) 3,552–3,572; and (3′) 3,904–3,921. All 3′ primers incorporated the universal primer sequence for subsequent dye–primer sequence analysis. The HIV-1 copy number in every PCR reaction was determined (100–10,000 copies). A total of three to six separate PCR amplifications of primary patient material was done on each sample using different combinations of primers, and representative chromatograms are shown. Rarely, codon interpretation was ambiguous. In the day +140 plasma sample from subject 1625 (bottom of panel *b*), the complementary (plus) strand could read: AGC(serine), GCN(alanine), ACN(threonine), AGA/AGG(arginine) or GGN(glycine). In this case, we sequenced 7 full-length RT molecular clones and found that they encoded only serine or alanine. For sequencing, an automated ABI 373A sequenator and the Taq Dye Primer Cycle Sequencing Kit (ABI) were used. Sequences were analysed using Sequencher (Gene Codes Corp.) and Microgenie (Beckman) software packages, and base-pair mixtures were quantified by measuring relative peak-on-peak heights[28].

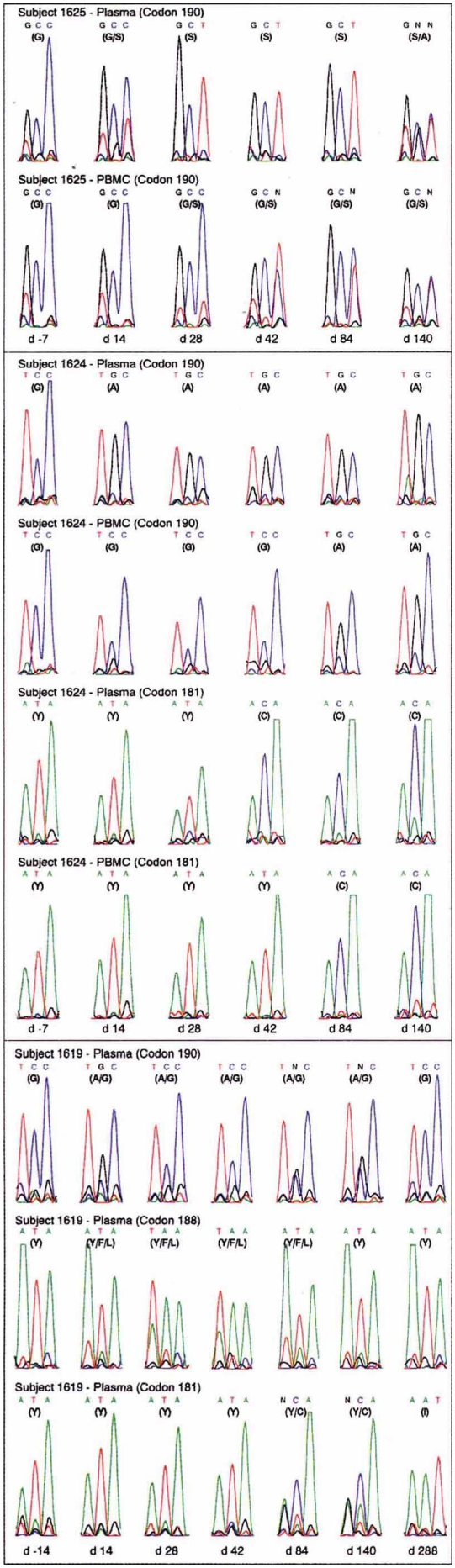


In all four subjects evaluated by direct viral population sequencing (Fig. 4), specific NVP-resistance-conferring mutations within the RT gene could be unambiguously identified and subsequently confirmed by molecular cloning, expression and drug susceptibility testing. In all cases, mutant virus increased rapidly in the plasma and virtually replaced wild-type virus after only 2–4 weeks of NVP therapy (Fig. 2*c*). By analysing the rate of accumulation of resistant mutants in the plasma population, we could obtain an independent estimate of the turnover rate of free virus. The rise of drug-resistant mutant virus is influenced substantially by the preceding increase in the $CD4^+$ cell population (which provides additional resources for virus production[33]) and therefore follows complex dynamics. However, we could obtain an estimate of these dynamics by making simplifying assumptions. We assume that wild-type virus declines exponentially with a decay rate $\alpha$, and that the drug-resistant mutant increases exponentially with the rate $\beta$. Thus, the ratio of mutant to wild-type virus increases exponentially at the combined rate $\alpha + \beta$. Our genetic RNA (cDNA) data allow us to estimate this sum. Knowing $\alpha$ from our data on virus decline, we get $\beta \approx 0.27$, or a 32% daily virus production (average over 4 patients). Assuming that mutant virus rises exponentially, this corresponds to a doubling time of ~2 days, which is in excellent agreement with the measured elimination half-life of $2.0 \pm 0.9$ days for plasma virus (Figs 1 and 2*a*). Turnover of viral DNA from wild-type to drug-resistant mutant in PBMCs was delayed and less complete compared to plasma virus, reaching levels of only 50–80% of the total PBMC-associated viral DNA population by week 20 (Fig. 2*c*). Measurement of the time required for resistant virus to spread in the PBMC population allowed us also to estimate the half-life of infected PBMCs. After complete turnover of mutant virus in the plasma pool, we may assume that PBMCs infected with wild-type virus decline exponentially at a rate $d$, whereas cells infected by mutant virus are generated at a constant rate, but also decline exponentially at rate $d$. With these simplifying assumptions, the rate at which the frequency of resistant virus in the PBMC population increases provides an estimate for the parameter $d$ and hence for the half-life of infected PBMCs. We obtained a half-life of ~50–100 days. This means that the average half-life of infected PBMCs is very long and of the same order of magnitude as the half-life of uninfected PBMCs[34,35]. Based on the long half-life of PBMCs, and the fact that these cells harbour predominantly wild-type virus at a time (days 14–28) when most virus in plasma is mutant, we conclude that most PBMCs contribute comparatively little to plasma virus load. Instead, other cell populations, most probably in the lymphoreticular system[11,19,20], must be the major source of virus production.

Direct sequence analysis of viral nucleic acid revealed not only rapid initial turnover in viral populations but also continuing viral evolution with respect to drug resistance mutations. In subject 1625 (Fig. 4, top panel), wild-type virus in plasma was completely replaced after 28 days of NVP therapy by mutant virus

FIG. 4 Quantitative detection of HIV-1 drug resistance mutations by automated DNA sequencing in plasma viral RNA (cDNA) and PBMC-associated viral DNA populations before and after the initiation of NVP on day 0. As in Fig. 3, minus-strand sequences are shown together with single-letter amino-acid codes of the corresponding plus-strand sequence. Mixed bases approximating a 50/50 ratio are denoted as N.

METHODS. HIV-1 cDNA was prepared from virions pelleted from uncultured plasma as described for Fig. 3. Viral DNA was isolated from uncultured PBMCs, as described[44]. The full-length viral reverse transcriptase genes as well as subgenomic fragments were amplified and sequenced as described for Fig. 3. The HIV-1 copy number in every PCR reaction was determined (100–10,000 copies). Some sequences were determined from both coding and non-coding DNA strands to ensure the accuracy of quantitative measurements.

TABLE 1 *In situ* functional analysis of HIV-1 RT clones

| Subject | Specimen | | Functional clones | NVP-sensitive clones | | NVP-resistant clones | |
|---|---|---|---|---|---|---|---|
| 1625 | Plasma | day −7 | 80 | 80 | (100%) | 0 | (0%) |
| | | +14 | 72 | 27 | (38%) | 45 | (62%) |
| | | +28 | 57 | 0 | (0%) | 57 | (100%) |
| | | +84 | 67 | 0 | (0%) | 67 | (100%) |
| | | +140 | 86 | 0 | (0%) | 86 | (100%) |
| 1625 | PBMC | −7 | 163 | 163 | (100%) | 0 | (0%) |
| | | +14 | 121 | 121 | (100%) | 0 | (0%) |
| | | +28 | 258 | 134 | (52%) | 124 | (48%) |
| | | +84 | 133 | 43 | (32%) | 90 | (68%) |
| | | +140 | 261 | 65 | (25%) | 196 | (75%) |
| 1624 | Plasma | −7 | 19 | 19 | (100%) | 0 | (0%) |
| | | +14 | 34 | 4 | (12%) | 30 | (88%) |
| | | +28 | 79 | 6 | (8%) | 73 | (92%) |
| | | +140 | 27 | 0 | (0%) | 27 | (100%) |
| 1624 | PBMC | −7 | 24 | 24 | (100%) | 0 | (0%) |
| | | +14 | 34 | 29 | (85%) | 5 | (15%) |
| | | +28 | 52 | 42 | (81%) | 10 | (19%) |
| | | +140 | 87 | 26 | (30%) | 61 | (70%) |
| 1605 | PBMC | −7 | 31 | 31 | (100%) | 0 | (0%) |
| | | +140 | 31 | 11 | (35%) | 20 | (65%) |
| 1619 | Plasma | −14 | 79 | 79 | (100%) | 0 | (0%) |
| | | +28 | 41 | 0 | (0%) | 41 | (100%) |
| | | +140 | 38 | 0 | (0%) | 38 | (100%) |

Full-length RT genes were amplified by PCR from uncultured plasma and uncultured PBMCs as described in Fig. 3 legend. DNA products were cloned into the *EcoRI* and *HindIII* sites of the bacterial expression plasmid pLG18-1 (refs 29, 30). The expression plasmids were screened for the presence of functional RT and tested *in situ* for susceptibility to NVP inhibition at 3,000 nM (~50–75 fold greater than the $IC_{50}$)[24,31,32]. To ensure accuracy in distinguishing RT genes encoding NVP-resistant versus sensitive enzymes, and to confirm the identification of specific NVP-resistance-conferring RT mutations obtained by direct sequencing (Figs 3 and 4), we determined the complete nucleotide sequences of 21 cloned RT genes which had been phenotyped in the *in situ* assay (V.A.J. and G.M.S., submitted). There was complete concordance between the phenotypes and genotypes of these 21 clones with respect to NVP-resistance-conferring mutations, as well as complete concordance between direct viral population sequences and clone-derived sequences at NVP-resistance-conferring codons.

(G190S), which in turn evolved by day 140 into a mixture of G190S and G190A. In subject 1624 (Fig. 4, middle panel), two codon changes conferring NVP resistance occurred. A G190A substitution appeared in plasma virus at day 14 and a Y181C appeared at day 42. Similarly, in subject 1605 (not shown), a Y181C mutation appeared in plasma at day 14 and a Y188L mutation at day 28. The sequential changes in plasma virus were mirrored by similar changes in PBMCs at later timepoints. In subject 1619, the pattern of resistance changes was even more complex (Fig. 4, bottom panel). By day 14, approximately 70% of plasma virus contained a G190A mutation. By day +28, this mutant population was largely replaced by virus containing a Y188F/L substitution. By day 84, still another major shift in the viral quasispecies occurred, this time resulting in a population of viruses containing mutations at both Y181C and G190A. Finally, by day 288 the viral population in plasma consisted exclusively of a mutant exhibiting a single tyrosine-to-isoleucine substitution at position 181 (Y181I); mutations at codons 188 and 190 were not present in this virus population. All of these amino-acid substitutions at RT codons 181, 188 and 190 were shown in our *in situ* expression studies and by others[31,32,36] to confer high-level NVP resistance. The direct sequence analyses thus demonstrate that major changes in the HIV-1 quasispecies occur quickly and continuously in response to selection pressures and that these changes are reflected first and most prominently in the plasma virus compartment.

***In situ* RT gene expression and drug susceptibility testing.** Because direct sequence analysis of viral mixtures provides only semiquantitative information and does not distinguish between viruses with functional rather than defective RT genes, we employed another method for quantifying virus turnover in uncultured plasma and PBMC compartments. Full-length RT genes were amplified by polymerase chain reaction (PCR), cloned into pLG18-1, expressed in *Escherichia coli*, and tested individually for enzymatic function and NVP susceptibility by *in situ* assay[29,30] (Table 1). For subject 1625 at day −7, 100% (80/80) of RT clones from plasma and 100% (163/163) of RT clones from PBMCs expressed enzyme that was sensitive to NVP inhibition. By day 14, however, 62% of plasma-derived clones expressed enzyme that was resistant to NVP, and by days 28, 84 and 140, 100% were resistant. Conversely, at day 14, 0% of PBMC-derived clones expressed NVP-resistant enzyme, and even after 28, 84 and 140 days, only 48–75% of clones were resistant. Similar results were obtained for the other study subjects (Table 1). Thus, the kinetics of virus population turnover determined by a quantitative RT *in situ* expression assay corresponded closely with those determined by direct population sequencing (Fig. 2*c*).

**Infectious virus drug susceptibility testing.** Plasma and PBMCs are known to harbour substantial proportions of defective or otherwise non-infectious virus[6,37]. To determine whether the viral genomes represented in total viral nucleic acid (Fig. 4 and Table 1) corresponded to infectious virus with respect to NVP-resistance-conferring mutations, we co-cultivated PBMCs from three of the study subjects (1605, 1624, 1625) with normal donor lymphoblasts in order to establish primary virus isolates. The RT genes of these cultured viruses, obtained before and after therapy, were cloned (Fig. 3 and Table 1 legends) and sequenced in their entirety (V.A.J. and G.M.S., submitted). RT codons associated with NVP susceptibility were completely concordant in cultured and uncultured virus strains. Furthermore, the virus isolates exhibited NVP susceptibility profiles[38] consistent with their genotypes.

## $CD4^+$ lymphocyte dynamics

Changes in $CD4^+$ lymphocyte counts during the first 28 days of therapy could be assessed in 17 of our patients (Fig. 2*b* and data not shown). $CD4^+$ cell numbers increased in every patient by between 41 and 830 cells per $mm^3$. For the entire group, the average increase was $186 \pm 199$ cells per $mm^3$ (mean ± s.d.), or $268 \pm 319$% from baseline. As $CD4^+$ lymphocytes increase in numbers because of (1) exponential proliferation of $CD4^+$ cells in peripheral tissue compartments, and/or (2) constant (linear) production of $CD4^+$ cells from a pool of precursors, we analysed our data based on each of these assumptions. The average percentage increase in cell number per day (assumption (1)) was $5.0 \pm 3.1$% (mean ± 1 s.d.). The average absolute increase in cell number per day (assumption (2)) was $8.0 \pm 7.8$ cells $mm^{-3}$ $d^{-1}$. Given that peripheral blood contains only 2% of the total body lymphocytes[35] and that the average total blood volume is ~5 litres, an increase of 8 cells $mm^{-3}$ $d^{-1}$ implies an overall steady-state $CD4^+$ cell turnover rate (where increases equal losses) of $(50) \times (5 \times 10^6\ mm^3) \times (8\ cells\ mm^{-3}\ d^{-1})$, or $2 \times 10^9$ $CD4^+$ cells produced and destroyed each day.

## Discussion

Previously, it was shown that lymphoreticular tissues serve as the primary reservoir and site of replication for HIV-1 (refs 11, 19, 20) and that virtually all HIV-1-infected individuals, regardless of clinical stage, exhibit persistent plasma viraemia in the range of $10^2$ to $10^7$ virions per ml[6]. However, the dynamic contributions of virus production and clearance, and of $CD4^+$ cell infection and turnover, to the clinical 'steady-state' were obscure, although not unanticipated[22,23,39]. We show by virus quantitation and mutation fixation rates that the composite lifespan of plasma virus and of virus-producing cells is remarkably short ($t_{1/2} = 2.0 \pm 0.9$ days). This holds true for patients with $CD4^+$ lymphocyte counts as low as 18 cells per $mm^3$ and as high as 355 cells per $mm^3$ (Figs 1 and 2; G.M.S., unpublished). These findings were made in patients treated with three different antiretroviral agents having two entirely different mechanisms of action and using three different experimental approaches for assessing virus turnover. The viral kinetics thus cannot be

explained by a unique or unforeseen drug effect or a peculiarity of any particular virological assay method. Moreover, when new cycles of infection are interrupted by potent antiretroviral therapy, plasma virus levels fall abruptly by an average of 99%, and in some cases by as much as 99.99% (10,000-fold). This result indicates that the vast majority of circulating plasma virus derives from continuous rounds of *de novo* virus infection, replication and cell turnover, and not from cells that produce virus chronically or are latently infected and become activated. The identity and location of this actively replicating cell population is not known, but appears not to reside in the PBMC pool, consistent with prior reports[11,19,20]. Nevertheless, PBMCs traffic through secondary lymphoid organs and to some extent are in equilibrium with these cells[35]. It is thus possible that a small fraction of PBMCs[8,9,14–17], like a small fraction of activated lymphoreticular cells[20], could make an important contribution to viraemia.

The magnitude of ongoing virus infection and production required to sustain steady-state levels of viraemia is extraordinary: based on a virus $t_{1/2}$ of 2.0 days and first-order clearance kinetics ($v(t) = v(0)e^{-\alpha t}$, where $\alpha = 0.693/t_{1/2}$), 30% or more of the total virus population in plasma must be replenished daily. For a typical HIV-1-infected individual with a plasma virus titre equalling the pretreatment geometric mean in this study ($10^{5.5}$ RNA molecules per ml/2 RNA molecules per virion = $10^{5.2}$ virions per ml) and a plasma volume of 3 litres, this amounts to $(0.30) \times (10^{5.2}) \times (3 \times 10^3) = 1.1 \times 10^8$ virions per day (range for all 22 subjects, $2 \times 10^7$ to $7 \times 10^9$). Even this may be a substantial underestimate of virus expression because virions may be inefficiently transported from the interstitial extravascular spaces into the plasma compartment and viral protein expression alone (short of mature particle formation) may result in cytopathy or immune-mediated destruction. Because the half-life of cells producing the majority of plasma virus cannot exceed 2.0 days, at least 30% of these cells must also be replaced daily. In our patients, we estimated the rate of $CD4^+$ lymphocyte turnover to be, on average, $2 \times 10^9$ cells per day, or about 5% of the total $CD4^+$ lymphocyte population, depending on clinical stage. This rapid and ongoing recruitment of $CD4^+$ cells into a short-lived virus-expressing pool probably explains the abrupt increase in $CD4^+$ lymphocyte numbers that is observed immediately following the initiation of potent antiretroviral therapy, and suggests the possibility of successful immunological reconstitution even in late-stage disease if effective control of viral replication can be sustained.

The kinetics of virus and $CD4^+$ lymphocyte production and clearance reported here have a number of biological and clinical implications. First, they are indicative of a dynamic process involving continuous rounds of *de novo* virus infection, replication and rapid cell turnover that probably represents a primary driving force underlying HIV-1 pathogenesis. Second, the demonstration of rapid and virtually complete replacement of wild-type virus by drug-resistant virus in plasma after only 14–28 days of drug therapy is a striking example of the capacity of the virus for biologically relevant change. In particular, this implies that HIV-1 must have enormous potential to evolve in response to selection pressures as exerted by the immune system[39]. Although other studies[40–42] have provided some evidence that virus turnover occurs sooner in plasma than in PBMCs, our data show this phenomenon most clearly. A similar experimental approach involving the genotypic and phenotypic analysis of plasma virus could be helpful in identifying viral mutations and selection pressures involved in resistance to other drugs, immune surveillance and viral pathogenicity. Third, the difference in lifespan between virus-producing cells and latently infected cells (PBMCs) suggests that virus expression *per se* is directly involved in $CD4^+$ cell destruction. The data do not suggest an 'innocent bystander' mechanism of cell killing whereby uninfected or latently infected cells are indirectly targeted for destruction by adsorption of viral proteins or by autoimmune reactivities.

Although we have emphasized that most virus in plasma derives from an actively replicating short-lived population of cells, latently infected cells that become activated or chronically producing cells that generate proportionately less virus (and thus do not contribute substantially to the plasma virus pool) may nonetheless be important in HIV-1 pathogenesis. Based on *in situ* analysis[20], these cells far outnumber the actively replicating pool and the diversity of their constituent viral genomes represents a potentially important source of clinically relevant variants, including those conferring drug resistance. In future studies, it will be important not only to discern the specific elimination rates of free virus and of the most actively producing cells, but also the dynamics of virus replication and cell turnover in other cell populations and in patients at earlier stages of infection. Such information will be essential to developing a better understanding of HIV-1 pathogenesis and a more rational approach to therapeutic intervention. □

Received 22 November; accepted 16 December 1994.

1. Ho, D. D., Moudgil, T. & Alam, M. *New Engl. J. Med.* **321,** 1621–1625 (1989).
2. Coombs, R. W. *et al. New Engl. J. Med.* **321,** 1626–1631 (1989).
3. Saag, M. S. *et al. J. Infect. Dis* **164,** 72–80 (1991).
4. Clark, S. J. *et al. New Engl. J. Med.* **324,** 954–960 (1991).
5. Daar, E. S., Mougdil, T., Meyer, R. D. & Ho, D.D. *New Engl. J. Med.* **324,** 961–964 (1991).
6. Piatak, M. Jr *et al. Science* **259,** 1749–1754 (1993).
7. Piatak, M. *et al. Lancet* **341,** 1099 (1993).
8. Schnittman, S. M., Greenhouse, J. J., Lane, H. C., Pierce, P. F. & Fauci, A. S. *AIDS Res. Hum. Retrovir.* **7,** 361–367 (1991).
9. Michael, N. L., Vahey, M., Burke, D. S. & Redfield, R. R. *J. Virol.* **66,** 310–316 (1992).
10. Winters, M. A., Tan, L. B., Katzenstein, D. A. & Merigan, T. C. *J. clin. Microbiol.* **31,** 2960–2966 (1993).
11. Pantaleo, G. *et al. Proc. natn. Acad. Sci. U.S.A.* **88,** 9838–9842 (1991).
12. Connor, R. I., Mohri, H., Cao, Y. & Ho, D. D. *J. Virol.* **67,** 1772–1777 (1993).
13. Bagnarelli, P. *et al. J. Virol.* **66,** 7328–7335 (1992).
14. Bagnarelli, P. *et al. J. Virol.* **68,** 2495–2502 (1994).
15. Graziosi, C. *et al. Proc. natn. Acad. Sci. U.S.A.* **90,** 6405–6409 (1993).
16. Patterson, B. K. *et al. Science* **260,** 976–979 (1993).
17. Saksela, K., Stevens, C., Rubinstein, P. & Baltimore, D. *Proc. natn. Acad. Sci. U.S.A.* **91,** 1104–1108 (1994).
18. Cao, Y. *et al. AIDS Res. Hum. Retrovir.* (in the press).
19. Pantaleo, G. *et al. Nature* **362,** 355–358 (1993).
20. Embretson, J. *et al. Nature* **362,** 359–362 (1993).
21. Aoki-Sei, S. *et al. AIDS Res. Hum. Retrovir.* **8,** 1263–1270 (1992).
22. Coffin, J. M. *Curr. Top. Microbiol. Immun.* **176,** 143–164 (1992).
23. Wain-Hobson, S. *Curr. Opin. Genet. Dev.* **3,** 878–883 (1993).
24. Merluzzi, V. J. *et al. Science* **250,** 1411–1413 (1990).
25. Kempf, D. *et al. Proc. natn. Acad. Sci. U.S.A.* (in the press).
26. Vacca, J. P. *et al. Proc. natn. Acad. Sci. U.S.A* **91,** 4096–4100 (1994).
27. Mulder, J. *et al. J. clin. Microbiol.* **32,** 292–300 (1994).
28. Larder, B. A. *et al. Nature* **365,** 671–675 (1993).
29. Prasad, V. R. & Goff, S. P. *J. biol. Chem.* **264,** 16689–16693 (1989).
30. Saag, M. S. *et al. New Engl. J. Med.* **329,** 1065–1072 (1993).
31. Richman, D. D. *et al. Proc. natn. Acad. Sci. U.S.A.* **88,** 11241–11245 (1991).
32. Richman, D. D. *et al. J. Virol.* **68,** 1660–1666 (1994).
33. McLean, A. R. & Nowak, M. A. *AIDS* **6,** 71–79 (1992).
34. Michie, C., McLean, A., Alcock, C. & Beverley, P. C. L. *Nature* **360,** 264–265 (1992).
35. Sprent, J. & Tough, D. F. *Science* **265,** 1395–1400 (1994).
36. Balzarini, J. *et al. Proc. natn. Acad. Sci. U.S.A.* **91,** 6599–6603 (1994).
37. Meyerhans, A. *et al. Cell* **58,** 901–910 (1989).
38. Japour, A. J. *et al. Antimicrob. Agents Chemother.* **37,** 1095–1101 (1993).
39. Nowak, M. A. *et al. Science* **254,** 963–969 (1991).
40. Simmonds, P. *et al. J. Virol.* **65,** 6266–6276 (1991).
41. Smith, M. S., Koerber, K. L. & Pagano, J. S. *J. infect. Dis.* **167,** 445–448 (1993).
42. Zhang, Y.-M., Dawson, S. C., Landsman, D., Lane, H. C.& Salzman, N. P. *J. Virol.* **68,** 425–432 (1994).
43. Myers, G. K., Korber, B., Berzofsky, J. A. & Smith, R.F. *Human Retroviruses and AIDS 1993* (Los Alamos National Laboratory, New Mexico, 1993).
44. Shaw, G. M. *et al. Science* **226,** 1165–1171 (1984).

ACKNOWLEDGEMENTS. We thank the study participants; K. Squires, J. M. Kilby, M. Trechsel, L. DeLoach and the UAB 1917 Clinic staff; Abbott Laboratories, Merck & Co. and Boehringer Ingelheim Pharmaceuticals Inc. (BIPI); J. Coffin, R. May and F. Gao for discussion; J. Decker, S. Campbell-Hill, Y. Niu and S. Yin Jiang for technical assistance; and J. Wilson for artwork. This study was supported by the NIH, the US Army Medical Research Acquisition Activity, BIPI, the Wellcome Trust, Keble College and Boehringer Ingelheim Stiftung. Core research facilities were provided by the UAB Center for AIDS Research, the UAB AIDS Clinical Trials Unit and the Birmingham Veterans Administration Medical Center.